Supersonic Low-Density Flow Over Airfoils

Tsze C. Tai* and Mark S. Moran†
David Taylor Research Center, Bethesda, Maryland 20084-5000

Two-dimensional, Reynolds-averaged, full Navier-Stokes equations for a perfect gas are solved for supersonic, low-density flow at Reynolds numbers ranging from 4×10^2–3.5×10^4. Slip-velocity boundary conditions based on various Knudsen numbers are introduced. This formulation is referred to as the extended Navier-Stokes method. Numerical results are obtained for three symmetric airfoils (NACA 0009, NACA 0012, and a 9%-thick, circular-arc airfoil) traveling at supersonic speeds at an angle of attack of 1.25 deg. The effect of the slip velocity becomes noticeable when the Knudsen number is greater than 0.01 and becomes important for $Kn > 0.1$. In a low-density atmosphere, the airfoil lift coefficients are low and drag coefficients are high because of strong viscous effects. The effect of the slip velocity tends to reduce both the lift and drag coefficients, but to a much smaller degree than the effect due to viscosity.

Nomenclature

a = speed of sound
c = chord length of an airfoil
e = total energy normalized by $\rho_\infty a_\infty^2$
h = altitude
Kn = Knudsen number
$\overline{Kn}$ = mean Knudsen number
M = Mach number
Pr = Prandtl number
p = $(\gamma - 1)[e - 0.5\rho(u^2 + v^2)]$
Re = Reynolds number
t = time
U, V = contravariant velocities
u, v = velocity components normalized by the freestream speed of sound a_∞
x, y = Cartesian coordinates normalized by the chord length
α = angle of attack
γ = specific heat ratio
δ = boundary-layer thickness
λ = mean free path
μ = dynamic viscosity
ν = kinematic viscosity
ξ, η = generalized curvilinear coordinates
ρ = gas density normalized by its freestream value
σ = diffuse reflection
τ = shear stress

Subscripts

s = slip condition
w = at wall
∞ = freestream condition

Introduction

CURRENT interest in high-altitude flight has prompted new exploration of low-density aerodynamics. Unfortunately, the theoretical models and computational capabilities developed to date have proven insufficient to characterize these flows fully. The difficulty has to do with the high degree of rarefaction of the flow. The low-density flows of interest occur in a transitional flow region between the continuum flow region and the molecular flow region. In this "transition region," the concept of transport coefficients (which are the basis for the Navier-Stokes equations) becomes invalid. Thus, the traditional Navier-Stokes analysis ceases to give accurate results. The objective of this research is to investigate the flow physics of high-altitude flight, and to develop a new computational scheme for assessing vehicle performance in this important flow regime.

In order to achieve sufficient lift for level flight, a high-altitude vehicle must fly at high speeds. A typical flight envelope would include freestream Mach numbers between 3 and 15, at an altitude of 30–50 miles above sea level. This flight regime, although considerably beyond the capability of existing aircraft, lies within the flight envelope of the National Aerospace Plane (X-30). The aerodynamic challenge is to achieve sufficiently high lift coefficients, at the prescribed altitudes but at a relatively low Mach number, so that certain hypersonic flow problems (such as heat transfer, chemical reactions, and surface catalytic activities) can be circumvented. In the present work, a hypothetical, infinite-span wing traveling at Mach numbers between 3 and 5 (corresponding to Reynolds numbers ranging from 3.6×10^2–5.3×10^4) is used as a test case. The infinite span allows the problem to be treated two-dimensionally.

In contrast with continuum flow, transition flow requires a higher-order approximation to the Boltzmann equation. Numerical solution to the Boltzmann equation consists of 1) the evaluation of the collision integral and 2) the integration of the differential equation. Although the integral form of the collision term causes much of the mathematical difficulty in solving the Boltzmann equation, the use of the velocity space coordinates as independent variables in partial differential equations requires large amounts of computer time and storage. The advent of high-speed computers has spurred the development of numerical solutions to the Boltzmann equation for several basic, one-dimensional cases.[1]

For flight altitudes of 30–50 miles above sea level, the flow is in the slip-flow regime, such that $M/\sqrt{Re}$ lies between 0.01 and 0.2. Two alternate approaches to solving the Boltzmann equation can be considered. The first approach is an extension of the continuum Navier-Stokes method to the slip-flow problem. For less rarefied slip flows, the Knudsen number (which characterizes rarefied gas dynamics) is small, and the rarefaction effects are mixed with strong compressibility and viscous effects. The continuum Navier-Stokes approach may be extended to the slip-flow problem by replacing the usual nonslip

Presented as Paper 89-0530 at the AIAA 27th Aerospace Sciences Meeting, Reno, NV, Jan. 9–12, 1989; received March 11, 1989; revision received July 6, 1989.

*Senior Research Scientist, Aircraft Division, Aviation Department. Associate Fellow AIAA.

†Aerospace Engineer, Aircraft Division, Aviation Department. Member AIAA.

condition in the flow calculation by a finite slip velocity at the wall. This procedure is of practical interest and might be superior for the range of Reynolds numbers being considered.

Another alternate approach to solving the Boltzmann equation is the direct simulation of the physics of the gas flow.[2] If the simulation of the collision phenomenon is consistent with the Boltzmann formulation, it can also yield the Boltzmann solution. First applied by Bird to the problem of translational flow,[3] the intermolecular collisions in the direct simulation technique are treated on a probabilistic basis with the aid of the Monte Carlo method. The technique, referred to as the direct simulation Monte Carlo (DSMC) method, requires the assumption of molecular chaos and is restricted to dilute gas flows in which the mean spacing between the molecules is large in comparison to the molecular diameter. Because the DSMC method avoids the use of velocity space coordinates, more complex problems can be treated with this technique.[4-6]

In the present paper, the methodology and results of the first approach are presented. The extended Navier-Stokes method has the distinct advantage of making use of recently advanced computational fluid dynamics capabilities, and should be adequate for the range of Reynolds numbers being considered. The DSMC method can serve as validation and assessment of the extended Navier-Stokes method, in the absence of adequate experimental data.

Extended Navier-Stokes Method

Governing Equations

The two-dimensional Navier-Stokes equations for a perfect gas written in generalized curvilinear coordinates (τ,ξ,η) are

$$\partial_t \hat{Q} + \partial_\xi \hat{E} + \partial_\eta \hat{F} = Re^{-1}(\partial_\xi \hat{E}_v + \partial_\eta \hat{F}_v) \tag{1}$$

$$\hat{Q} = J^{-1}\begin{bmatrix}\rho\\ \rho u\\ \rho v\\ e\end{bmatrix}, \qquad \hat{E} = J^{-1}\begin{bmatrix}\rho U\\ \rho uU + \xi_x p\\ \rho vU + \xi_y p\\ U(e+p) - \xi_t p\end{bmatrix}$$

$$\hat{F} = J^{-1}\begin{bmatrix}\rho V\\ \rho uV + \eta_x p\\ \rho vV + \eta_y p\\ V(e+p) - \eta_t F\end{bmatrix} \tag{2}$$

with the contravariant velocities

$$U = \xi_t + \xi_x u + \xi_y v, \qquad V = v_t + \eta_x u + \eta_y v$$

The viscous flux terms are $\hat{E}_v = J^{-1}(\xi_x E_v + \xi_y F_v)$ and $\hat{F}_v = J^{-1}(\eta_x E_v + \eta_y F_v)$, where

$$E_v = \begin{bmatrix}0\\ \tau_{xx}\\ \tau_{xy}\\ f\end{bmatrix}, \qquad F_v = \begin{bmatrix}0\\ \tau_{xy}\\ \tau_{yy}\\ g\end{bmatrix} \tag{3}$$

with

$$\tau_{xx} = \mu(4u_x - 2v_y)/3 \tag{4a}$$

$$\tau_{xy} = \mu(u_y + v_x) \tag{4b}$$

$$\tau_{yy} = \mu(-2u_x + 4v_y)/3 \tag{4c}$$

$$f = u\tau_{xx} + v\tau_{xy} + \mu Pr^{-1}(\gamma-1)^{-1}\partial_x a^2 \tag{4d}$$

$$g = u\tau_{xy} + v\tau_{yy} + \mu Pr^{-1}(\gamma-1)^{-1}\partial_y a^2 \tag{4e}$$

The metric terms are defined as

$$\xi_x = Jy_\eta, \qquad \xi_y = -Jx_\eta, \qquad \xi_t = -x_\tau\xi_x - y_\tau\xi_y$$

$$\eta_x = -Jy_\xi, \qquad \eta_y = Jx_\xi, \qquad \eta_t = -x_\tau\eta_x - y_\tau\eta_y \tag{5}$$

$$J^{-1} = (x_\xi y_\eta - x_\eta y_\xi) \tag{6}$$

Boundary conditions are as follows: for outer boundaries, the flow is undisturbed, i.e., $U = u = M_\infty$, $V = v = 0$, and $\rho = 1$; at the body surface, the viscous conditions apply, i.e., $U = V = 0$.

Equations (1) and (2) are the Reynolds-averaged, Navier-Stokes equations of the continuum theory. Thus far, there has been no departure from the conventional continuum approach. The preceding system follows the development of Pulliam[7] and Steger.[8] However, the "thin-layer" approximation of Ref. 7 has not been undertaken here.

Slip Velocity Boundary Condition

In solving the Navier-Stokes equations for a low-density flow, a departure is made from the conventional continuum approach in that the usual nonslip conditions at the wall are now replaced with slip conditions. This approach is justified for flows with low Reynolds numbers in which the rarefaction effects are mixed with strong compressibility and viscous effects. The Knudsen number Kn, which is defined as the ratio of the length of the molecular mean free path to some significant dimension of the flowfield, is not much smaller than unity. Such flows lie in the slip-flow regime, somewhere be-

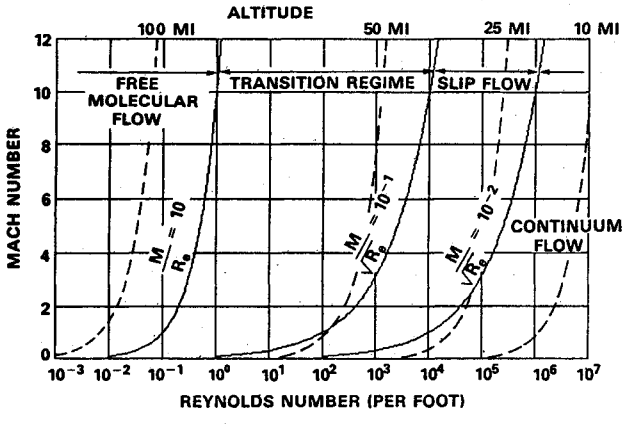

Fig. 1 Regimes of gas dynamics.

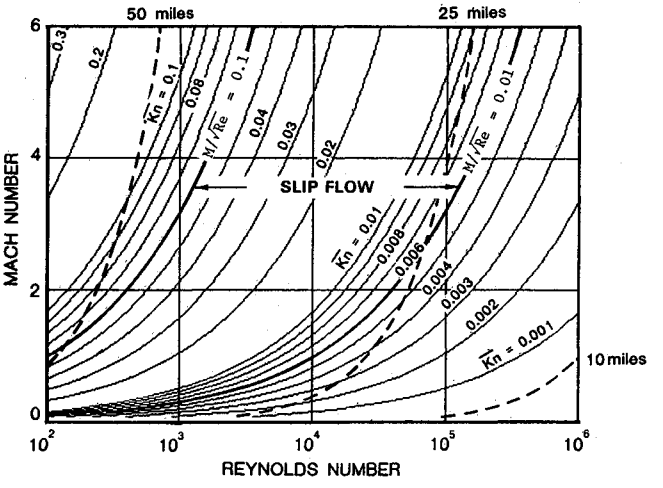

Fig. 2 Knudsen number values in slip-flow regime.

tween the continuum flow and the transition flow; see Fig. 1.

When the Reynolds number is not too small, i.e., $Re \gg 1$, the significant characteristic dimension of the flow is the boundary-layer thickness.[9] Since the boundary-layer thickness is inversely proportional to the square root of the Reynolds number, for a laminar boundary layer, the slip-flow regime is defined by the following limits[9]:

$$0.01 < M/\sqrt{Re} < 0.1 \qquad \text{for } Re \gg 1$$

By the same token, the Knudsen number is given by[9]

$$Kn = \lambda/\delta \tag{7}$$

where λ is defined as[9]

$$\lambda = 1.26\sqrt{\gamma}\,(\nu/a) \tag{8}$$

and δ is approximated by

$$\delta = \frac{5x}{\sqrt{Re_x}} \tag{9}$$

Substituting Eqs. (8) and (9) into Eq. (7) yields the expression for the local Knudsen number:

$$Kn = \frac{0.298\,M_\infty}{\sqrt{x/c}\,\sqrt{Re}} \tag{10}$$

Equation (10) indicates that the local Knudsen number at the leading edge can be much larger than that at the trailing edge.

Accordingly, the mean Knudsen number for the entire airfoil is given by

$$\overline{Kn} = \int_0^1 \frac{0.298\,M_\infty}{\sqrt{x/c}\,\sqrt{Re}}\,d(x/c) = 0.596\,\frac{M_\infty}{\sqrt{Re}} \tag{11}$$

The mean Knudsen number is equal to the local Knudsen number at the quarter chord, $x/c = \frac{1}{4}$. Values of the mean Knudsen number in the Mach number and Reynolds number range of interest are plotted in Fig. 2.

Because there are no large-scale deviations from the continuum behavior in the slip-flow regime, the flowfield is still generally governed by the continuum equations. The rarefaction effects may be taken into account by applying the slip conditions between the flowfield and the body surface. Since the heat-transfer problem is not addressed in the present work, the slip condition corresponds to a velocity slip only. No temperature jump is considered.

Because of the interactions between the gas molecules and the body surface, determination of the slip flow velocity with kinetic theory is fairly difficult. However, for engineering purposes, an approximate analysis based on a monatomic gas adjacent to an isothermal surface serves to relate the slip velocity and the gradient of the tangential velocity[9]:

$$U_s = \frac{2-\sigma}{\sigma}\,Kn\left(\frac{\partial U}{\partial \eta}\right)_w \tag{12}$$

where

$$\left(\frac{\partial U}{\partial \eta}\right)_w = (\xi_y u_\xi + \eta_y u_\eta)_w \tag{13}$$

The Cartesian velocities are related to the contravariant velocities through the following transformation:

$$\begin{pmatrix} u \\ v \end{pmatrix} = J^{-1}\begin{bmatrix} \eta_y & -\xi_y \\ -\eta_x & \xi_x \end{bmatrix}\begin{pmatrix} U_s - \xi_t \\ 0 - \eta_t \end{pmatrix} \tag{14}$$

For flows with Reynolds numbers ranging from 4×10^2–3.5×10^4, the boundary layer remains laminar; hence, only laminar flow is considered.

Numerical Solution

An implicit, approximate factorization, finite-difference scheme is employed in solving the partial differential equations represented by Eq. (1). Local time linearizations are applied to the nonlinear terms, and an approximate factorization of the two-dimensional implicit operator is used to produce block tridiagonal matrices. The spatial derivative terms are approximated with second-order central differences. Explicit and implicit artificial dissipation terms are added to achieve nonlinear stability. The numerical procedure uses the ARC2D code developed by Pulliam[7] and Steger,[8] except that the full Navier-Stokes equations are used in the present work, rather than the thin-layer equations employed in the standard ARC2D program.

Both slip and nonslip boundary conditions for velocity are applied at the wall. Of course, the nonslip condition produces the conventional continuum solution. Equation (12) is used to evaluate the slip velocity. Full diffuse reflection (i.e., $\sigma = 1$) is assumed.

Results and Discussion

Numerical results are obtained at altitudes ranging from 28–50 miles above sea level for three airfoils: NACA 0009 and NACA 0012 airfoils, and a 9%-thick, circular-arc airfoil. The low-density atmosphere condition requires a high flight speed (Mach 3–5) to achieve sufficient lift for level flight. The angle of attack of the airfoil is kept as low as possible to avoid high drag values. For these altitudes, the Reynolds number ranges from 5.3×10^4–3.6×10^2. This corresponds to a Knudsen number range of 0.02–0.2, which lies in the slip-flow regime. Numerical "C" grids are used for all three airfoils.[10] For the preceding Reynolds number range, the boundary layer remains laminar; hence, only laminar flow is considered.

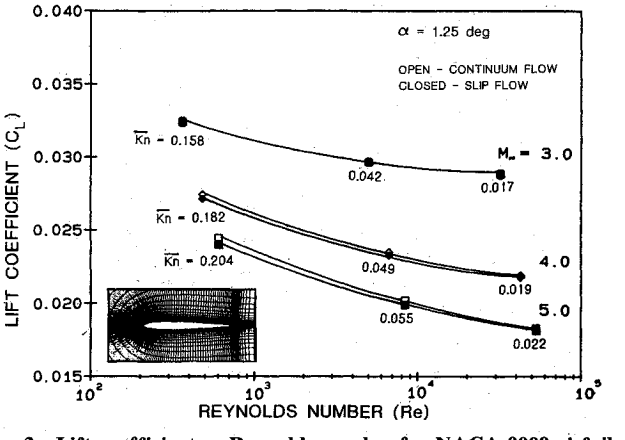

Fig. 3 Lift coefficient vs Reynolds number for NACA 0009 airfoil.

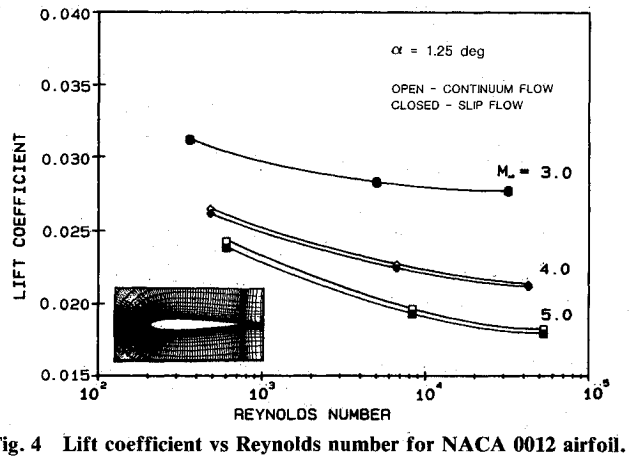

Fig. 4 Lift coefficient vs Reynolds number for NACA 0012 airfoil.

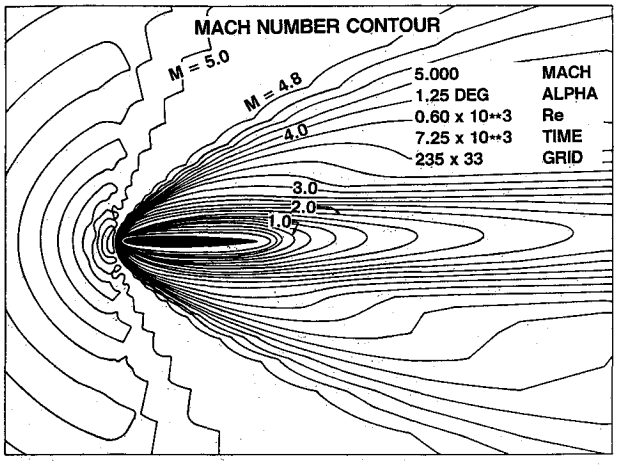

Fig. 5 Mach number contours around NACA 0009 airfoil at $M_\infty = 5.0$, $\alpha = 1.25$ deg, and $h = 50$ miles.

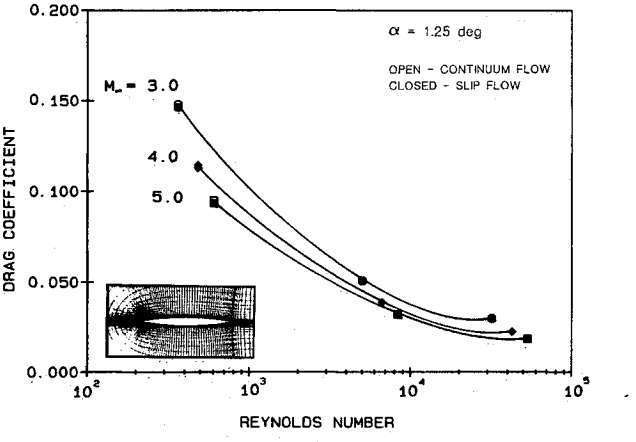

Fig. 7 Drag coefficient vs Reynolds number for 9%-thick, circular-arc airfoil.

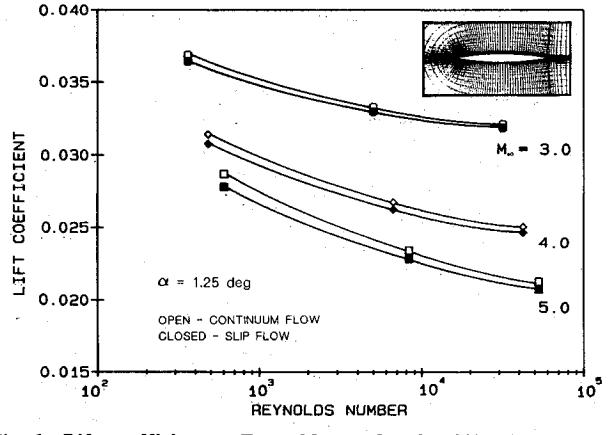

Fig. 6 Lift coefficient vs Reynolds number for 9%-thick, circular-arc airfoil.

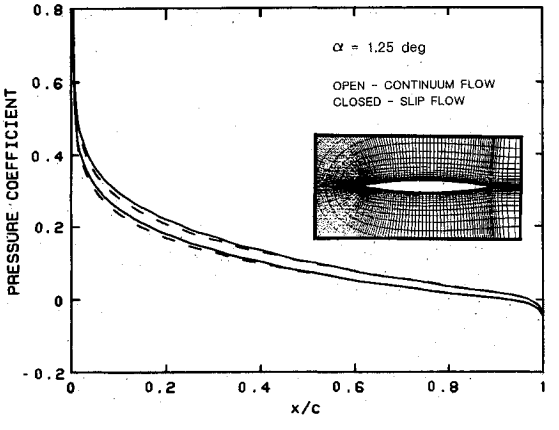

Fig. 8 Pressure distribution over 9%-thick, circular-arc airfoil at $M_\infty = 4.0$ and $\alpha = 1.25$ deg.

Results are presented in terms of aerodynamic lift and drag coefficients of these airfoils at altitudes of 28, 38, and 50 miles. Figure 3 shows lift coefficient vs Reynolds number for the NACA 0009 airfoil at $M_\infty = 3$, 4, and 5, and $\alpha = 1.25$ deg, with both the slip and nonslip (continuum) conditions applied. The lift coefficient increases moderately as the Reynolds number decreases (altitude increases). Ordinarily, the lift coefficient would be expected to decrease with decreasing Reynolds numbers or increasing rarefaction. In the present results, however, the flow is totally laminar. A decrease in Reynolds number enhances the laminar mixing and thus decreases the pressure in the suction side (upper surface), which leads to a higher lift coefficient. The physics here are similar to those in the case of base pressure. Kavanau[11] found from the measurements in a low Reynolds number range ($Re < 1 \times 10^4$) that the base pressure on a cone-cylinder body decreases monotonically as the Reynolds number decreases.

The local mean Knudsen numbers are indicated at various data points. The effect of the slip velocity on the lift coefficient becomes noticeable for Knudsen numbers greater than 0.01, but is important for $Kn > 0.1$. There is a slight decrease in lift when the slip condition is applied. Unfortunately, available experimental data[12] are rather limited for comparison purposes. This increase in lift coefficient with increasing altitude also applies to the case of an NACA 0012 airfoil, for which lift coefficient vs Reynolds at $M_\infty = 3$–5 is shown in Fig. 4.

The Mach number contour over an NACA 0009 airfoil at $M_\infty = 5$, $\alpha = 1.25$ deg, and $h = 50$ miles is shown in Fig. 5. The detached shock wave in front of the leading edge forces the velocity to go subsonic. The extensive subsonic region near the surface of the airfoil suggests that a very thick laminar boundary layer has developed, which causes excessive form drag and thus leads to a high drag coefficient.

Circular-arc airfoils, or their derivatives such as parabolic-arc airfoils or conical-section airfoils, are considered to be efficient airfoils for supersonic flight.[13] In the present work, a 9%-thick, circular-arc airfoil is used as a representative test case. For the same flow conditions and airfoil thickness, the lift coefficient of the circular-arc airfoil at various Reynolds numbers is about 12% higher than that of the NACA 0009 airfoil (see Fig. 6). Once again, the slip effect becomes important when the Knudsen number is greater than 0.1. In general, the lift coefficient increases slightly as the altitude increases, although it is adversely affected by the slip condition.

The airfoil drag coefficient rises sharply with increasing altitude. Figure 7 shows drag coefficient vs Reynolds number for the 9%-thick, circular-arc airfoil traveling at $M_\infty = 3$–5 and $\alpha = 1.25$ deg. The drag rise is due to the presence of a very thick laminar boundary layer which develops in low-density flows. The rate of the drag increase, however, is slightly attenuated by the slip effect. When the slip condition is applied, the stress is reduced, which leads to a lower skin friction than that determined by the traditional continuum theory. Similar effects in very low Reynolds number flows have been found by Moss et al.[4] on blunt bodies of revolution using the DSMC method.

The pressure distribution over the 9%-thick, circular-arc airfoil at $M_\infty = 4$ and $\alpha = 1.25$ deg, with slip and nonslip conditions applied, is shown in Fig. 8. Toward the forward

half of the airfoil, there is a slight shift of the pressure curve, due to the addition of the slip velocity given by Eq. (12). The effect of slip velocity diminishes toward the trailing edge of the airfoil.

Concluding Remarks

The continuum Navier-Stokes method for solving airfoil flows has been extended to the slip-flow regime by replacing the usual nonslip boundary condition with the slip velocity at the wall. Numerical results on low-density flows over three airfoils indicate that the effect of slip velocity becomes noticeable when the Knudsen number is greater than 0.01 and becomes important for $Kn \geq 0.1$. In a low-density atmosphere, the airfoil lift coefficients are low and drag coefficients are high because of strong viscous effects. The addition of the slip velocity tends to reduce both the lift and drag coefficients, but to a much smaller degree than the effects due to viscosity. The overall lift-to-drag ratio is almost unchanged by the slip effect.

Although it is more rigorous to pursue a direct solution to the Boltzmann equation for the slip flow problem, the present extended Navier-Stokes method appears to be quite appropriate for the range of Knudsen numbers and Reynolds numbers considered.

Acknowledgments

This work was supported by the Independent Research Program at the David Taylor Research Center (WU 1660-115). The Cray computer time was provided by the NASA Ames Research Center. The authors are grateful to S. M. Yen and K. Lee of the University of Illinois and T. H. Pulliam and T. L. Holst of the NASA Ames Research Center for their helpful discussions concerning the present method.

References

[1]Yen, S. M., "Numerical Solution of the Nonlinear Boltzmann Equation for Nonequilibrium Gas Flow Problems," *Annual Review of Fluid Mechanics,* Vol. 16, 1984, pp. 67–97.

[2]Bird, G. A., "Monte Carlo Simulation of Gas Flows," *Annual Review of Fluid Mechanics,* Vol. 10, 1978, pp. 11–31.

[3]Bird, G. A., "Approach to Translational Equilibrium in a Rigid Sphere Gas," *Physics of Fluids,* Vol. 6, Oct. 1963, pp. 1518–1519.

[4]Moss, J. N., Cuda, V., Jr., and Simmonds, A. L., "Nonequilibrium Effects for Hypersonic Transitional Flows," AIAA Paper 87-0404, Jan. 1987.

[5]Dogra, V. K., Moss, J. N., and Simmonds, A. L., "Direct Simulation of Stagnation Streamline Flow for Hypersonic Reentry," AIAA Paper 87-0405, Jan. 1987.

[6]Hermina, W. L., "Monte Carlo Simulation of Rarefied Flow Along a Flat Plate," AIAA Paper 87-1547, June 1987.

[7]Pulliam, T. H., "Euler and Thin Layer Navier-Stokes Codes: ARC2D, ARC3D," Notes for Computational Fluid Dynamics User's Workshop, Univ. of Tennessee Space Inst., Tullahoma, TN, March 1984.

[8]Steger, J. L., "Implicit Finite-Difference Stimulations of Flow about Arbitrary Geometries with Application to Airfoils," AIAA Paper 77-665, Jan. 1977.

[9]Schaaf, S. A. and Chambre, P. L., "Flow of Rarefied Gases," *High Speed Aerodynamics and Jet Propulsion,* Vol. 3, Sec. H, Princeton Univ. Press, Princeton, NJ, 1958, pp. 687–739.

[10]Cordova, J. Q. and Barth, T., "Grid Generation for General Two-Dimentional Regions Using Hyperbolic Equations," AIAA Paper 88-0520, Jan. 1988.

[11]Kavanau, L. L., "Base Pressure Studies in Rarefied Supersonic Flow," *Journal of the Aeronautical Sciences,* Vol. 23, March 1956, pp. 193–208.

[12]Allegre, J., Raffin, M., and Gottesdiener, L., "Slip Effects on Supersonic Flowfields Around NACA 0012 Airfoils," *Proceedings of the 15th International Symposium on Rarefied Gas Dynamics,* Vol. I, edited by V. Boff and C. Cercignani, B. G. Teubner, Stuttgart, Germany, 1986, pp. 548–557.

[13]Pittman, J. L., "Supersonic Airfoil Optimization," *Journal of Aircraft,* Vol. 24, Dec. 1987, pp. 873–880.